Contributions to Geophysics and Geodesy Vol. 39/1, 2009 (1–17)

Global maps of the step-wise topography corrected and crustal components stripped geoids using the CRUST 2.0 model

Robert TENZER[1], HAMAYUN[2], Peter VAJDA[3]

[1] School of Surveying, Faculty of Sciences, University of Otago
310 Castle Street, Dunedin, New Zealand; e-mail: robert.tenzer@surveying.otago.ac.nz

[2] Delft Institute of Earth Observation and Space Systems (DEOS), Delft University of Technology
Kluyverweg 1, 2629 HS Delft, The Netherlands; e-mail: K.Hamayun@tudelft.nl

[3] Geophysical Institute of the Slovak Academy of Sciences
Dúbravská cesta 9, 845 28 Bratislava, Slovak Republic; e-mail: Peter.Vajda@savba.sk

Abstract: We compile global maps of the step-wise topography corrected and crustal components stripped geoids based on the geopotential model EGM'08 complete to spherical harmonic degree 180 and the CRUST 2.0 global crustal model. The spectral resolution complete to degree 180 is used to compute the primary indirect bathymetric stripping and topographic effects on the geoid, while degree 90 for the primary indirect ice stripping effect. The primary indirect stripping effects of the soft and hard sediments, and the upper, middle and lower consolidated crust components are forward modeled in spatial form using the 2×2 arc-deg discrete data of the CRUST 2.0 model. The ocean, ice, sediment and consolidated crust density contrasts are defined relative to the adopted reference crustal density of 2670 kg/m^3. Finally we compute and apply the primary indirect stripping effect of the density contrast (relative to the mantle) of the reference crust. The constant value of -520 kg/m^3 is adopted for this density contrast relative to the mantle. All data are evaluated on a 1×1 arc-deg geographical grid. The complete crust-stripped geoidal undulations, globally having a range of approximately 1.5 km, contain the gravitational signal coming from the global mantle lithosphere (upper mantle) morphology and density composition, and from the sub-lithospheric density heterogeneities. Large errors in the complete crust-stripped geoid are expected due to uncertainties of the CRUST 2.0 model, i.e., due to deviations of the CRUST 2.0 model density from the real earth's crustal density and due to the Moho-boundary uncertainties.

Key words: forward modeling, stripping, interpretation, geoid, crust, isostasy

1. Introduction

In gravimetry the technique known as "stripping" is used when a part of the earth subsurface mass-density distribution is known (in terms of a model produced as a result of other geoscientific investigations), and its gravitational effect is removed from the observed field, in order to unmask the remaining gravitational signal of the unknown (and sought) anomalous subsurface density distribution. Stripping is typically applied to gravity anomalies or gravity disturbances. However, with the same objective, it may be applied to geoidal undulations, deflections of the vertical, or second derivatives of the disturbing potential. Here we focus on stripping the geoid on a global scale. To quote some studies that have applied the stripping technique to the global geoid, we refer to (e.g., *Dahlen, 1981; Lister, 1982; Chase and McNutt, 1982; Hager, 1983; Le Stunff and Ricard, 1995; Kaban et al., 1999; 2004*). The global stripped geoid studies typically use an "isostatic residual geoid", which is essentially a "lithosphere-stripped geoid" adopting a model isostatically compensated lithosphere produced by a particular least-squares inversion scheme with apriori data on the crustal density composition and the Moho boundary. The lithosphere-stripped geoid is then interpreted to study the sub-lithospheric mantle density heterogeneities and mantle dynamics. For instance *Kaban et al. (1999)* compute and interpret a global lithosphere-stripped geoid in spectral form complete to degree and order 30, based on the satellite only geoid solution of the GRIM4-S4 *(Schwintzer et al., 1997)* and the global crustal data of the CRUST 5.1 model *(Mooney et al., 1998)*. Similarly, *Kaban et al. (2004)* use a global lithosphere-stripped geoid based on the geoid complete to spherical harmonic degree 180 of the EGM'96 geopotential model and crustal data of the CRUST 2.0 model *(Bassin et al., 2000)*.

We focus here on a purely crust-stripped global geoid. We strip from the global geoid complete to spherical harmonic degree 180 of the EGM'08 geopotential model *(Pavlis et al., 2008a; 2008b)* the effects (in geodesy referred to as 'primary indirect effects') of the structural crust components of the CRUST 2.0 model. First we remove from the geoid the primary indirect topographic effect, which is equivalent to applying the topographic correction to gravity data. Second we strip the geoid of the primary indirect effect of the global ocean water density contrast (relative to the reference crustal

density of 2670 kg/m^3), this being equivalent to applying the bathymetric correction to gravity data. Next we strip, step-by-step, the geoid of the primary indirect effects of the density contrasts of the global CRUST 2.0 crustal components of ice, sediments, and consolidated crust down to the Moho boundary. The ice, sediment and consolidated crust density contrasts are defined relative to the reference crustal density of 2670 kg/m^3.

In regional geophysical studies investigating the lithosphere structure (e.g., *Bielik, 1988; Artemjev and Kaban, 1994; Artemjev et al., 1994; West et al., 1995; Kaban 2001; 2002; Bielik et al., 2004; Braun et al., 2007; Tassara et al., 2007; Tesauro et al., 2007; Alvey et al., 2008; Jiménez-Munt et al., 2008;* and others) geoidal heights are sometimes used along with gravity data as constraining information, or in integrated forward modeling (e.g., *Zeyen et al., 2002; Dérerová et al., 2006*). In such cases the same effects must be removed from both the gravity and the geoid, in order to preserve the equivalence. For instance the topography corrected geoid is equivalent to the Bouguer gravity, or the crust-stripped geoid is equivalent to the crust-stripped gravity data. Also, in large regional studies, the stripping corrections should be computed globally, since their distant-zone component may significantly contribute to the long-wavelength part of the interpreted data in the given region that in turn reflect on the deep crustal and lithospheric lateral density heterogeneities.

The CRUST 2.0 model is available for the scientific community (`http://mahi.ucsd.edu/Gabi/rem.dir/crust/crust2.html`) and contains information on global subsurface spatial density distribution, with 2×2 arc-deg resolution, of the following global crustal components: ice, soft and hard sediments, upper, middle and lower consolidated crust. Following the removal of the primary indirect topographic and bathymetric effects from the geoidal heights, we apply the ice, sediment, and consolidated crust stripping corrections to the geoid in two subsequent steps. First these crustal stripping corrections are applied to the geoidal heights with the respective density contrasts defined relative to the reference crustal density of 2670 kg/m^3. The resulting consolidated crust-stripped geoid is hence respective to a model earth of no topography, a constant 2670 kg/m^3 crust in-between the bounding surfaces of the reference ellipsoid and the Moho boundary, and the real density below the Moho boundary. Second the primary indirect stripping effect of the reference crust density contrast (relative

to the mantle) is subtracted from the consolidated crust-stripped geoid. The reference crust density contrast relative to the mantle of -520 kg/m^3 was found by minimising the correlation between the Moho relief and the gravity field (cf. *Tenzer et al., 2009*). The resulting complete crust-stripped geoid represents a model earth of no topography, a constant density of 3190 kg/m^3 in-between the bounding surfaces of the reference ellipsoid and the Moho boundary, and the real density below the Moho boundary.

2. Primary indirect topographic and crust-stripping effects

The 5×5 arc-min global elevation data from the ETOPO5 (provided by the NOAA's National Geophysical Data Centre) were used to generate the Global Elevation Model coefficients. These coefficients were utilized to compute globally the primary indirect topographic effect with a spectral resolution complete to degree and order 180. The average topographic density 2670 kg/m^3 was adopted (cf. *Hinze, 2003*) in computing the topography-generated gravitational potential. An expression for modeling the gravitational potential from the spectral coefficients can be found for instance in *Vaníček et al. (1995)* and *Novák and Grafarend (2006)*. The primary indirect topographic effect is shown in Fig. 1, and statistics are given in Table 1. The maxima are located in the mountainous regions and the minima over the oceanic areas.

The 5×5 arc-min global bathymetry data from the ETOPO5 were used to generate the Global Bathymetric Model coefficients. These coefficients were utilized to compute globally the primary indirect bathymetric stripping effect with a spectral resolution complete to degree and order 180. The mean value of the ocean density contrast –1640 kg/m^3 (i.e., the difference between the mean ocean saltwater density 1030 kg/m^3 and the reference crustal density 2670 kg/m^3) was adopted. The primary indirect bathymetric stripping effect is shown in Fig. 2, and statistics are given in Table 1. The highest negative values are located over the central parts of the Pacific, Indian and Atlantic Oceans, and the lowest negative values in the central Eurasia.

The discrete data of the ice thickness with a 2×2 arc-deg geographical resolution from the CRUST 2.0 were used to generate the Global Ice Thickness Model coefficients. The ice thickness and elevation coefficients were

Table 1. Statistics of the primary indirect effects to the complete crust-density contrast stripped geoid

Primary indirect effect due to	Min [m]	Max [m]	Mean [m]	STD [m]
Topography	241	905	389	119
Ocean density contrast	-2908	-1670	-2280	325
Ice density contrast	-357	-32	-76	75
Sediment density contrast	-319	-164	-229	40
Consolidated crust density contrast (relative to reference density of 2670 kg/m^3)	3308	5637	4271	595
Reference crust density contrast (relative to mantle)	-7706	-5088	-6148	650

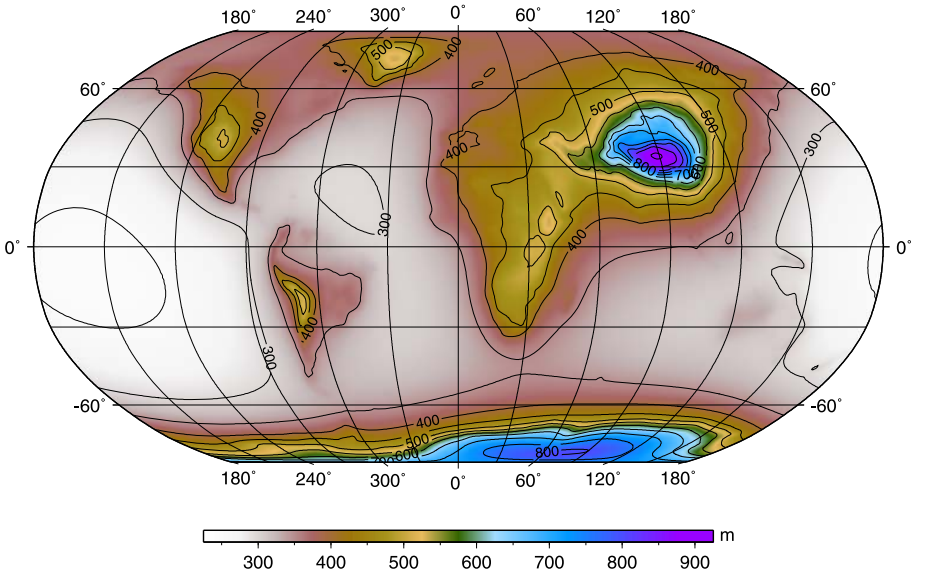

Fig. 1. The primary indirect topographic effect.

utilized to compute globally the primary indirect ice stripping effect with a spectral resolution complete to degree and order 90. The mean value of the ice density contrast –1757 kg/m^3 (i.e., the difference between the mean ice density 913 kg/m^3 and the reference crustal density 2670 kg/m^3) was adopted. The primary indirect ice stripping effect is shown in Fig. 3, and statistics are given in Table 1. The highest negative values correspond to

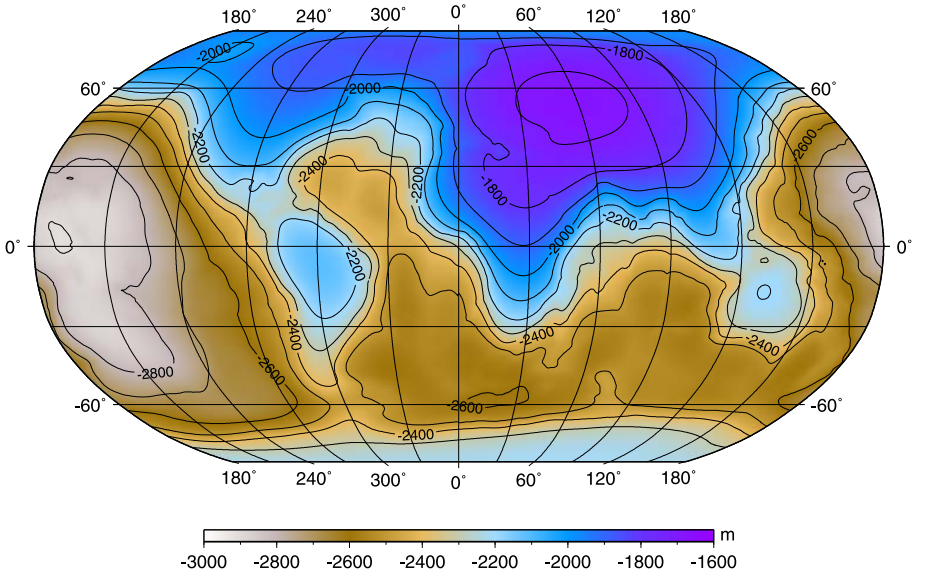

Fig. 2. The primary indirect bathymetric stripping effect.

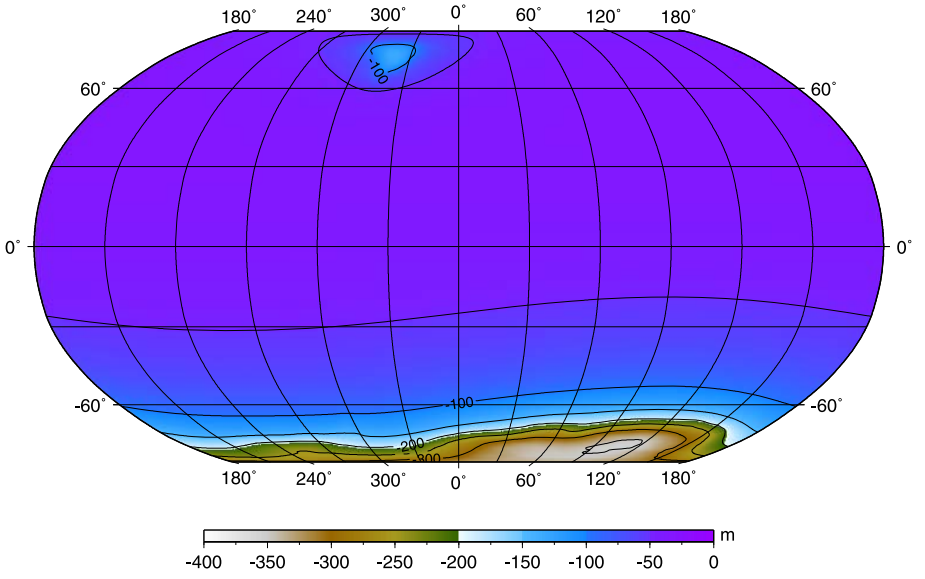

Fig. 3. The primary indirect ice stripping effect.

locations of the largest thickness of the polar ice sheet in Greenland and Antarctica.

The 2×2 arc-deg discrete data of the soft and hard sediment thickness and density from the CRUST 2.0 were used to compute globally in spatial representation the primary indirect sediment stripping effect. The CRUST 2.0 soft and hard sediment model components have the varying (cell to cell) lateral density of the sediments. The soft sediments vary in density from 1700 to 2300 kg/m^3 and reach a maximum thickness of about 2 km, while the hard sediments vary between 2300 and 2600 kg/m^3 and become up to 18 km thick at places. The sediment density contrast was defined relative to the reference crustal density 2670 kg/m^3. The primary indirect sediment stripping effect is shown in Fig. 4, and statistics are given in Table 1. The highest negative values are located over the areas with the largest sediment deposits in the continental shelves, the Caspian Sea region, and across the central Eurasia. The lowest negative values are across central parts of the Pacific, Atlantic, and Indian Oceans.

The 2×2 arc-deg discrete data of the density and thickness of the upper, middle, and lower consolidated crust components of the CRUST 2.0

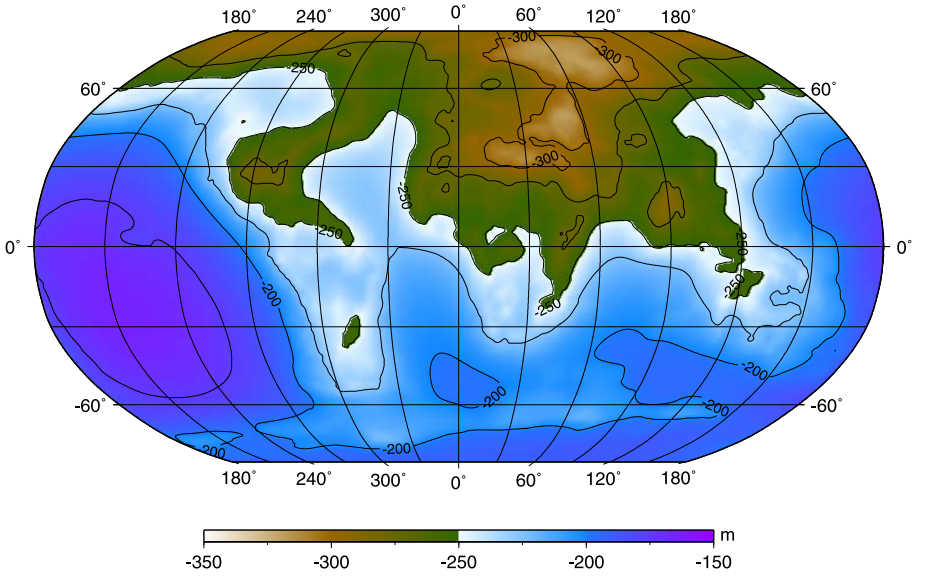

Fig. 4. The primary indirect sediment stripping effect.

model were used to compute globally in spatial representation the primary indirect stripping effect due to the density contrast of the remaining consolidated crust down to the Moho boundary. The upper crust component laterally varies in density from 2600 to 2800 kg/m^3 with a thickness ranging from 1.7 to 25 km. The middle crust component laterally varies in density from 2800 to 2900 kg/m^3 with a thickness ranging from 2.3 to 25 km. The lower crust component laterally varies between 2900 and 3100 kg/m^3 and has a thickness ranging from 2.5 to 25 km. The density contrasts of the three consolidated crustal components are defined relative to the reference crustal density of 2670 kg/m^3. The primary indirect stripping effect of the consolidated crust density contrast (relative to the reference crustal density of 2670 kg/m^3) is shown in Fig. 5, and statistics are given in Table 1. The maxima are located over the continental regions with the largest depths of the Moho boundary and large anomalous density variations (relative to the reference crustal density) within the consolidated crust. The minima are across central parts of the Pacific, Atlantic, and Indian Oceans.

The 2×2 arc-deg discrete data of the depth of the Moho boundary from the CRUST 2.0 were used to compute globally the primary indirect striping effect due to the density contrast relative to the mantle of the reference crust in-between the reference ellipsoid and the Moho boundary. The constant density contrast of the reference crust relative to the encompassing mantle of -520 kg/m^3 was adopted. The choice of this value is justified in Section 3. The primary indirect stripping effect of the reference crust density contrast (relative to the mantle) is shown in Fig. 6, and statistics are given in Table 1. The highest negative values correspond with the areas of the largest CRUST 2.0 model crust thickness, and the lowest negative values are across central parts of the Pacific, Atlantic, and Indian Oceans.

3. Global maps of the step-wise and complete crust-stripped geoids

The global geopotential coefficients taken from the EGM'08 complete to degree and order 180 were used to compute the geoidal heights. The computation was realized globally at the 1×1 arc-deg geographical grid. The expressions for computing the quantities of the gravity field in terms of

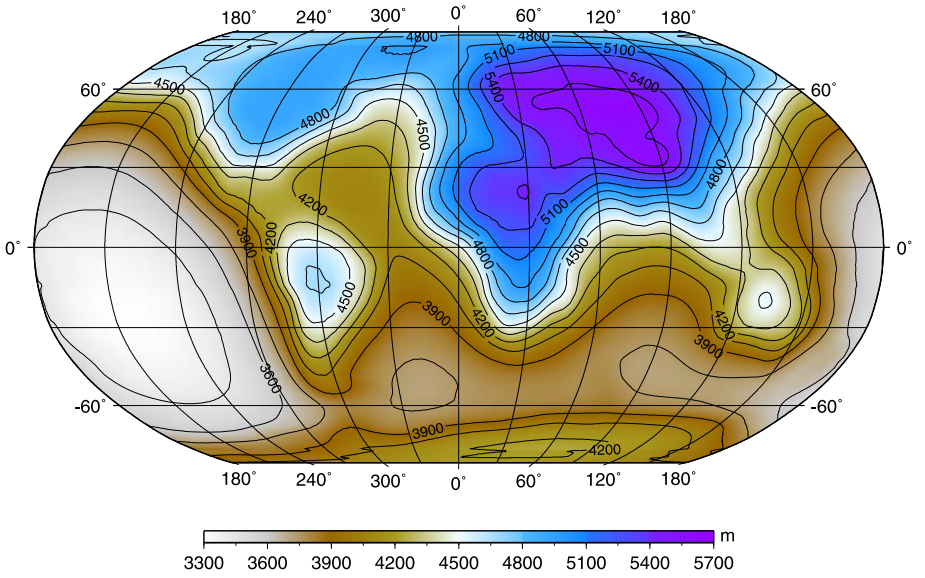

Fig. 5. The primary indirect stripping effect of the consolidated crust density contrast relative to the reference crustal density of 2670 kg/m^3.

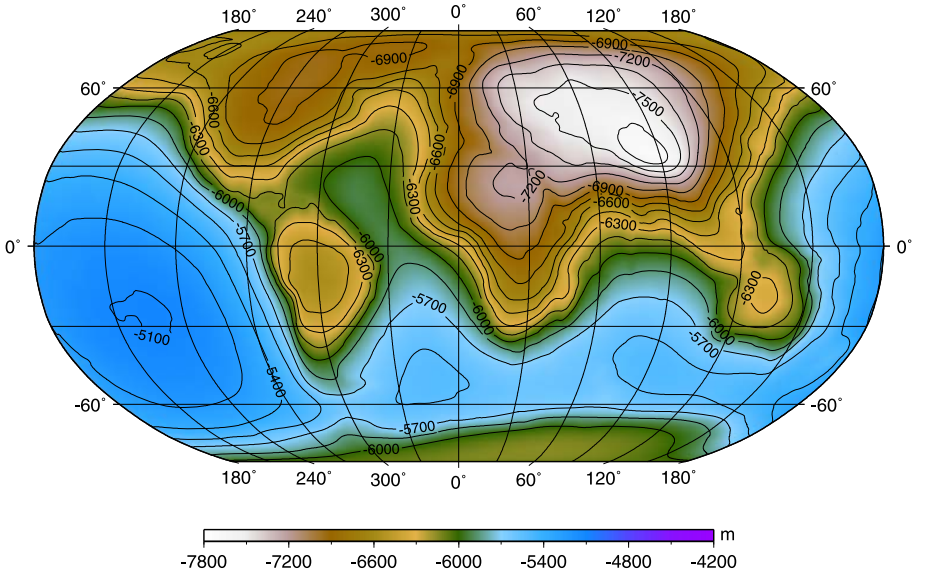

Fig. 6. The primary indirect stripping effect of the reference crust density contrast relative to the mantle.

spherical harmonics can be found for instance in Heiskanen and *Moritz (1967*, chapter 2-17). The geoid is shown in Fig. 7, and statistics are given in Table 2. The geoidal heights range from –106 to 85 m. The step-wise complete crust-stripped geoids were obtained from the geoidal heights by subsequent applications of the individual primary indirect effects (i.e., gravitational potentials multiplied by a reciprocal value of the normal gravity evaluated at the reference ellipsoid) of Section 2. Statistics of the step-wise complete crust-stripped geoids are summarized in Table 2.

The topographically corrected geoid was obtained from the geoidal heights after subtracting the primary indirect topographic effect. The topographically corrected geoid is everywhere negative (below the reference geocentric ellipsoid GRS'80) and varies from –940 to –188 m (cf., Fig. 8). Compared to the geoid, the topographically corrected geoid changed significantly especially in the mountainous regions.

The bathymetrically stripped and topographically corrected (BT) geoid was obtained from the topographically corrected geoid after subtracting the primary indirect bathymetric stripping effect. The BT geoid is everywhere positive and varies from 832 to 2678 m (cf., Fig. 9). Compared to the topographically corrected geoid, maximal changes of the BT geoid are over the oceanic areas.

The ice and sediment stripped BT geoid was obtained from the BT geoid after subtracting the primary indirect ice and sediment stripping effects. The ice and sediment stripped BT geoid is everywhere positive and varies from 1122 to 2886 m (cf., Fig. 10). Compared to the primary indirect bathymetric stripping and topographic effects, the signature of the primary indirect ice and sediment stripping effects is less noticeable. The application of the primary indirect ice stripping effect changed the BT geoid over the regions with the largest thickness of the polar ice sheet of Greenland and Antarctica. The application of the primary indirect sediment stripping effect primarily changed the BT geoid over the areas with the largest sediment thickness at continental shelves, the Caspian Sea region, and across the central Eurasia.

The application of the primary indirect effect of the consolidated crust density contrast (relative to the reference crustal density) to the ice and sediment stripped BT geoid transforms the volumetric domains of the upper, middle, and lower CRUST 2.0 crustal components from their laterally

Table 2. Statistics of the step-wise and complete crust-stripped geoids

Geoid	Min [m]	Max [m]	Mean [m]	STD [m]
Earth's	-106	85	-1	29
Topographically corrected	-940	-188	-390	129
BT	832	2678	1891	400
Ice and sediment stripped BT	1122	2886	2196	363
Consolidated crust-stripped (relative to 2670 kg/m^3)	-4489	-466	-2075	946
Complete crust-stripped (relative to mantle)	3215	4713	4073	308

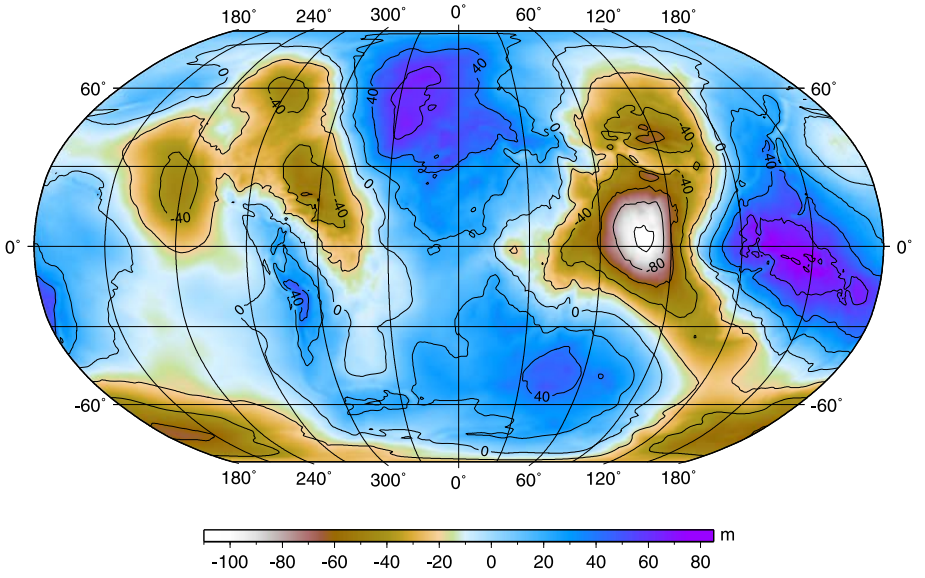

Fig. 7. The geoid computed with a spectral resolution complete to degree 180 of spherical harmonics.

varying densities to the constant reference density of 2670 kg/m^3. When this effect is subtracted from the ice and sediment stripped BT geoid, it produces the geoid that corresponds to a model earth consisting of no topography, a constant 2670 kg/m^3 reference density crust down to the Moho boundary, and the real earth's sub-Moho density distribution. We have

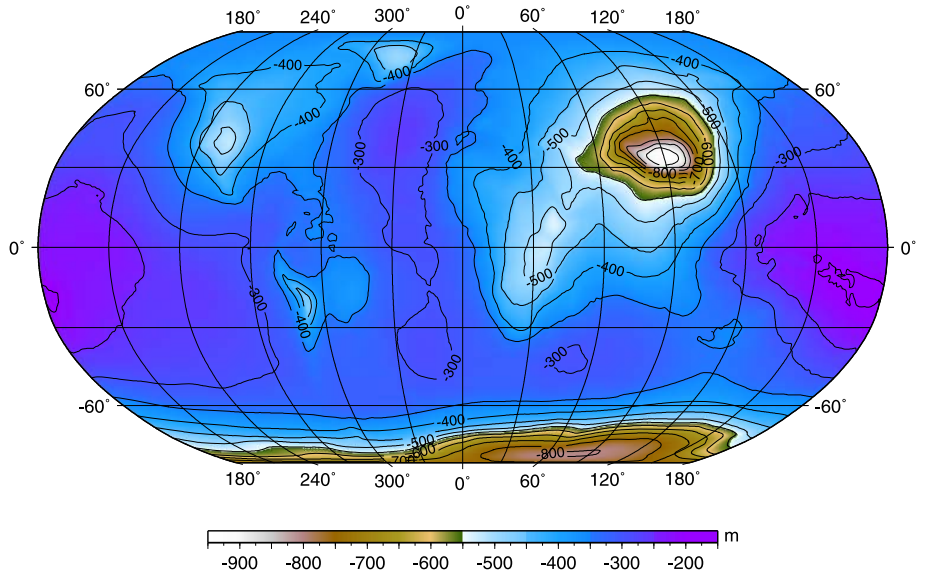

Fig. 8. The topographically corrected geoid.

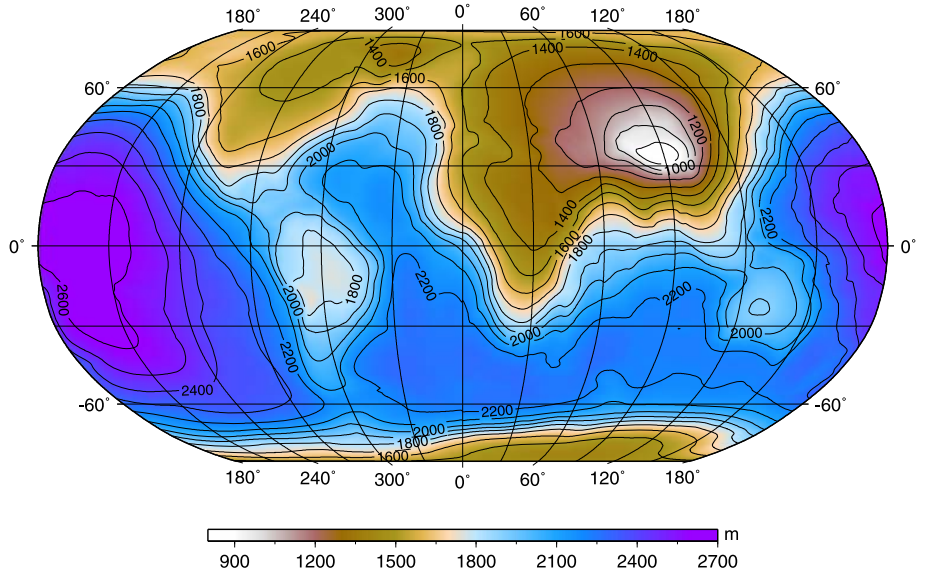

Fig. 9. The topographically corrected and bathymetrically stripped (BT) geoid.

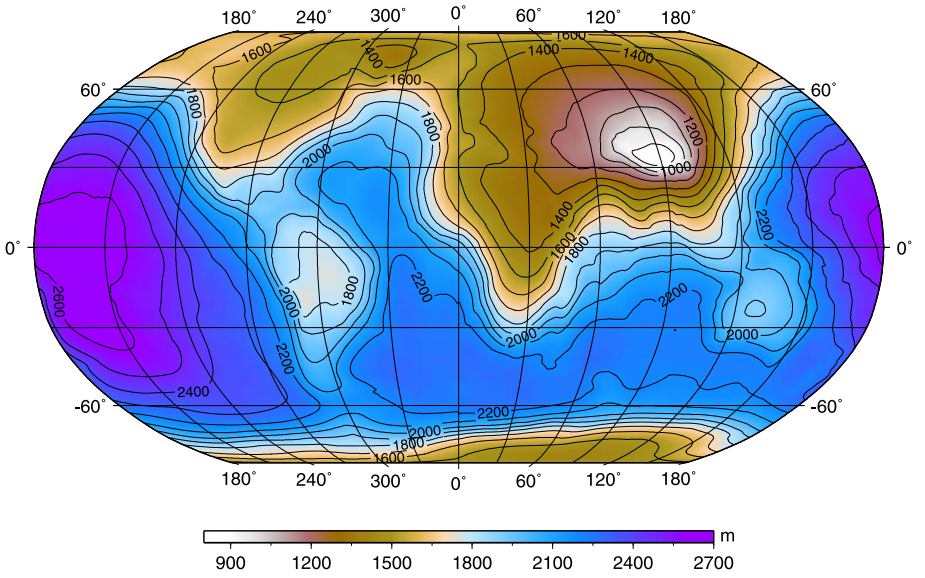

Fig. 10. The ice and sediment stripped BT geoid.

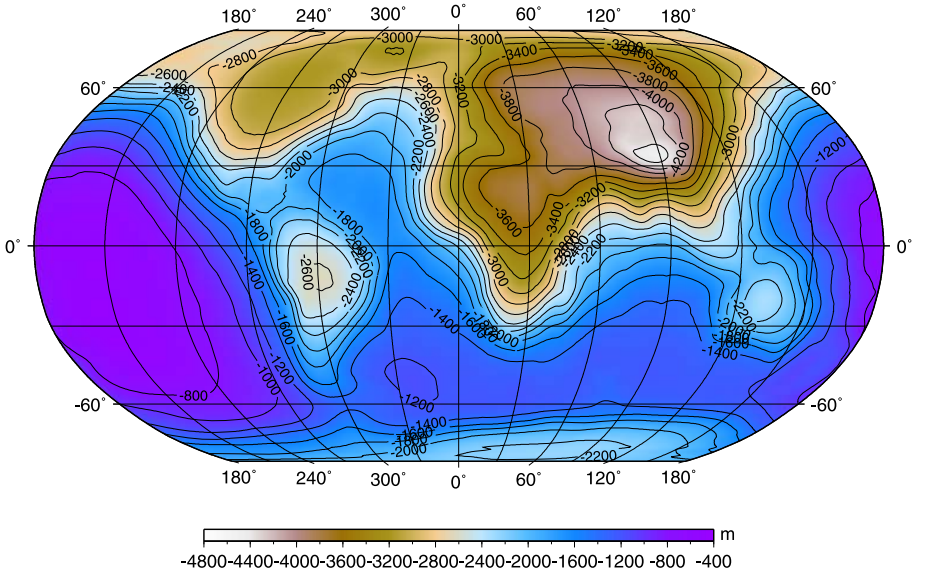

Fig. 11. The consolidated crust-stripped (relative to the reference crustal density of 2670 kg/m^3) geoid.

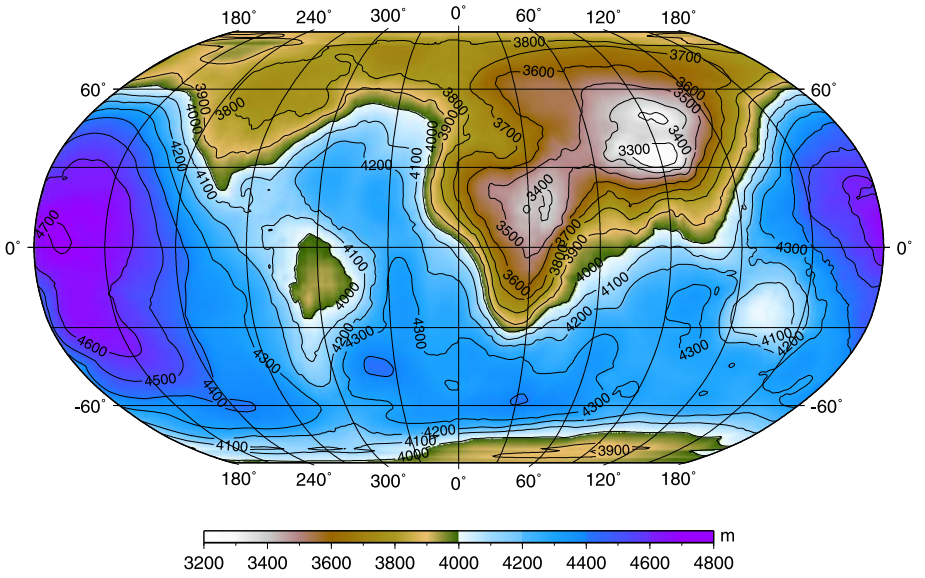

Fig. 12. The complete crust-stripped (relative to mantle) geoid.

called this geoid the "consolidated crust-stripped geoid". The consolidated crust-stripped geoid is everywhere negative and varies from –4489 to –466 m (cf., Fig. 11).

In the next and herein final step, we subtracted from the consolidated crust-stripped geoid the primary indirect effect of the constant reference crust density contrast relative to the mantle. For this purpose we first estimated the value of the density contrast of the reference crust relative to a constant (unspecified) mantle density, by minimizing the correlation of the compete crust-stripped gravity disturbances with the Moho boundary. This has been done by a trial-and-error method; cf., *Tenzer et al. (2009)*. The zero-correlation was reached at -520 kg/m^3. This final stripping step results in the complete crust-stripped geoid, which is everywhere positive and varies from 3215 to 4713 m (cf., Fig. 12). This geoid should ideally contain only the gravitational signal of density inhomogeneities and density contrast interfaces bellow the Moho boundary. Large errors are however expected due to the deviations of the CRUST 2.0 model density from the real earth's crustal density heterogeneities and the CRUST 2.0 Moho-relief

uncertainties.

4. Summary and conclusions

We have computed the global geoidal heights corrected for the global primary indirect topographic effect, and the global primary indirect stripping effects due to the major known density contrasts within the earth's crust based on the CRUST 2.0 model and the global geopotential model EGM'08 complete to spherical harmonic degree 180. The "consolidated crust-stripped" geoidal undulations represent (ideally) the gravity field generated by a model earth of no topography, a constant density of 2670 kg/m^3 in the volumetric domain in-between the surfaces of the reference ellipsoid and the Moho boundary, and a real density distribution below the Moho boundary. The "complete crust-stripped" geoidal undulations represent (ideally) the gravity field generated by a model earth of no topography, a constant density of 3190 kg/m^3 in the volumetric domain in-between the surfaces of the reference ellipsoid and the Moho boundary, and a real density distribution below the Moho interface.

The complete crust-stripped geoid (Fig. 12), globally having a range of approximately 1.5 km, when compared to the (observed) geoid (Fig. 7) with a global range of 200 m, is a clear indicator of the fact that the isostatic compensation does not take place within the earth's crust only, but its significant part takes place in the upper mantle (mantle lithosphere, lithospheric mantle), cf. also *Kaban et al. (1999, 2004)*. The complete crust-stripped geoid contains information coming from the global upper mantle morphology and density composition (reflecting global past and present tectonics with respective thermal and stress fields and the tendency toward isostatic balance), and from the sub-lithospheric (deeper mantle) density anomalies (reflecting the lithosphere-mantle interactions and the mantle convection). However, the crust-stripped geoid also contains a still significant contribution of the crustal model uncertainties caused by deviations of the CRUST 2.0 model density from the real earth's crustal density.

Acknowledgments. Peter Vajda was partially supported by the VEGA grant agency under projects No. 2/0107/09 and 1/0461/09.

References

Alvey A., Gaina C., Kusznir N. J., Torsvik T. H., 2008: Integrated crustal thickness mapping and plate reconstructions for the high Arctic. Earth Planet Sci. Lett., **274**, 310–321.

Artemjev M. E., Kaban M. K., 1994: Density inhomogeneities, isostasy and flexural rigidity of the lithosphere in the Transcaspian region. Tectonophysics, **240**, 281–297.

Artemjev M. E., Kaban M. K., Kucherinenko V. A., Demjanov G. V., Taranov V. A., 1994: Subcrustal density inhomogeneities of the Northern Euroasia as derived from the gravity data and isostatic models of the lithosphere. Tectonophysics, **240**, 248–280.

Bassin C., Laske G., Masters G., 2000: The current limits of resolution for surface wave tomography in North America. EOS, Trans AGU, **81**, F897.

Bielik M., 1988: A preliminary stripped gravity map of the Pannonian Basin. Phys. Earth Planet Inter., **51**, 185–189.

Bielik M., Šefara J., Kováč M., Bezák V., Plašienka D., 2004: The Western Carpathians–interaction of Hercynian and Alpine processes. Tectonophysics, **393**, 63–86.

Braun A., Kim H. R., Csatho B., von Frese R. R. B., 2007: Gravity-inferred crustal thickness of Greenland. Earth Planet. Sci. Lett., **262**, 138–158.

Chase C. G., McNutt M. K., 1982: The geoid: effect of compensated topography and uncompensated oceanic trenches. Geophys. Res. Lett., **9**, 29–32.

Dahlen F. A., 1981: Isostasy and the ambient state of stress in the oceanic lithosphere. J. Geophys. Res., **86**, B, 7801–7807.

Dérerová J., Zeyen H., Bielik M., Salman K., 2006: Application of integrated geophysical modeling for determination of the continental lithospheric thermal structure in the eastern Carpathians. Tectonics, **25**, 3, doi: TC3009 10.1029/2005TC001883.

Hager B. H., 1983: Global isostatic geoid anomalies for plate and boundary layer models of the lithosphere. Earth Planet. Sci. Lett., **63**, 97–109.

Heiskanen W. H., Moritz H., 1967: Physical geodesy. San Francisco, WH Freeman and Co.

Hinze W. J., 2003: Bouguer reduction density, why 2.67? Geophysics, **68**, 5, 1559–1560, doi: 10.1190/1.1620629.

Jiménez-Munt I., Fernàndez M., Vergés J., Platt J. P., 2008: Lithosphere structure underneath the Tibetan Plateau inferred from elevation, gravity and geoid anomalies. Earth Planet. Sci. Lett., **267**, 276–289.

Kaban M. K., 2001: A gravity model of the north Eurasia crust and upper mantle: 1. Mantle and isostatic residual gravity anomalies. Russ. J. Earth Sci., **3**, 143–163.

Kaban M. K., 2002: A gravity model of the north Eurasia crust and upper mantle: 2. The Alpine-Mediterranean fold-belt and adjacent structures of the southern former USSR. Russ. J. Earth Sci., 4, http://www.agu.org/wps/rjes/.

Kaban M. K., Schwintzer P., Tikhotsky S. A., 1999: Global isostatic gravity model of the Earth. Geophys. J. Int., **136**, 519–536.

Kaban M. K., Schwintzer P., Reigber Ch., 2004: A new isostatic model of the lithosphere and gravity field. Journal of Geodesy, **78**, 368–385, doi: 10.1007/s00190-004-0401-6.

Le Stunff Y., Ricard Y., 1995: Topography and geoid due to lithospheric mass anomalies. Geophys. J. Int., **122**, 982–990.

Lister G. R. B., 1982: Geoid anomalies over a cooling lithosphere: source of a third kernel of upper mantle thermal parameters and thus an inversion. Geophys. J. R. Astr. Soc., **68**, 219–240.

Mooney W. D., Laske G., Masters T. G., 1998: CRUST 5.1: A global crustal model at $5^\circ \times 5^\circ$. J. Geophys. Res., 103B, 727–747.

Novák P., Grafarend E. W., 2006: The effect of topographical and atmospheric masses on spaceborne gravimetric and gradiometric data. Studia Geophys. Geod., **50**, 4, 549–582 doi: 10.1007/s11200-006-0035-7.

Pavlis N. K., Holmes S. A., Kenyon S. C., Factor J. K., 2008a: An Earth Gravitational Model to Degree 2160: EGM 2008, presented at Session G3: "GRACE Science Applications", EGU Vienna.

Pavlis N. K., Holmes S. A., Kenyon S. C., Factor J. K., 2008b: EGM2008: An Overview of its Development and Evaluation. Presented at IAG Int. Symp. GGEO 2008, 23–27 June 2008, Chania, Crete, Greece.

Schwintzer P., Reigber C., Bode A., Kang Z., Zhu SY., Massmann F. H., Raimondo J. C., Biancale R., Balmino G., Lemoine J. M., Moynost B., Marty J. C., Barlier F., and Boudon Y., 1997: Long-wavelength global gravity field models: GRIM4-S4, GRIM4-C4. Journal of Geodesy, **71**, 4, 189–208.

Tassara A., Swain Ch., Hackney R., Kirby J., 2007: Elastic thickness structure of South America estimated using wavelets and satellite-derived gravity data. Earth Planet. Sci. Lett., **253**, 17–36.

Tenzer R., Hamayun, Vajda P., 2009: Global maps of CRUST 2.0 crustal components stripped gravity disturbances. J. Geophys. Res. Solid Earth (accepted).

Tesauro M., Kaban M. K., Cloetingh S. A., Hardebol N. J., Beekman F., 2007: 3D strength and gravity anomalies of the European lithosphere. Earth Planet. Sci. Lett., **263**, 56–73.

Vaníček P., Najafi M., Martinec Z., Harrie L., Sjöberg L. E., 1995: Higher-degree reference field in the generalised Stokes-Helmert scheme for geoid computation. Journal of Geodesy, **70**, 176–180.

West B. P., Fujimoto H., Honsho Ch., Tamaki K., Sempéré J. C., 1995: A three-dimensional gravity study of the Rodrigues Triple Junction and Southeast Indian Ridge. Earth Planet. Sci. Lett., **133**, 175–184.

Zeyen H., Dérerová J., Bielik M., 2002: Determination of the continental lithosphere thermal structure in the Western Carpathians: Integrated modelling of surface heat flow, gravity anomalies and topography. Phys. Earth Planet. Inter., **134**, 89–104.